

## Behavior of Composite Steel-Concrete Beam Subjected To Negative Bending

Dr. Ikbal N. Korkess\* , Anas H. Yousifany\* , Dr. Qais Abdul-Majeed\*  
& Dr. Husain M. Husain\*

Received on: 4/9/2007

Accepted on: 3/4/2008

### Abstract

This work deals with the behavior of structural continuous composite steel-concrete beams, which are widely used in building and bridge constructions. Therefore the structural behavior of composite beams under negative moment is a significant subject. However experimental tests in this field are very rare and information about the efficiency of shear connection when the slab is under tension are really few.

In the present research, available experimental tests on composite steel-concrete beams under negative bending are theoretically analyzed using the finite element software ANSYS. ANSYS computer program is a large-scale multipurpose finite element program which may be used for solving several cases of engineering analyses.

The proposed three dimensional model is able to simulate the overall flexural behavior of composite beams. This covers; load-deflection behavior, longitudinal slip at the steel-concrete interface, and distribution of shear studs. The reliability of the model is demonstrated by comparison with available experiment and alternative numerical analysis which shows 9-10% difference.

**Keywords:** ANSYS, Composite beams, Finite Element Method, Negative moments, Partial interaction, slip, uplift

### سلوك الروافد المركبة من عتبات فولاذية وبلاطات خرسانية تحت الانحناء السالب

#### الخلاصة

الروافد المركبة المستمرة تتكون من بلاطات خرسانية وعتبات حديدية تربطها روابط باشكال مختلفة, وهي ذات استخدام واسع في الهندسة المدنية في مجالي الجسور وانشاء الابنية. لهذا فان دراسة تصرفها تحت العزوم السالبة اصبح امرا ضروريا. ان التجارب العملية في هذا المجال قليلة وان المعلومات عن سلوك البلاطات والروابط المعرضة الى قوى شد غير متوفرة الى حد ما. تضمن البحث تحليل نظري لنتائج عملية متوفرة للروافد المركبة المستمرة تحت تاثير العزوم السالبة وذلك باستخدام طريقة العناصر المحددة (برنامج جاهز ANSYS software). بالامكان استخدام البرنامج لحساب السلوك العام بكفاءة ودقة لمختلف مستويات التحميل ولغاية الفشل. ولقد اقترح موديل ( نموذج ) حسابي ثلاثي الابعاد للتحليل اللاخطي باستخدام هذا البرنامج. تم التحليل بتغطية الحمل-الهطول لسلوك المنشأ المركب، الانزلاق الطولي بين البلاطة الخرسانية والعتبة الحديدية وتوزيع رباطات القص. تمت المقارنة مع النتائج العملية المتوفرة. ولوحظ ان الاختلاف يتراوح بين 9-10%.

## Introduction

Composite steel-concrete construction, particularly for bridge superstructures and multi-story frames, has achieved a high market share in several countries. This is mainly due to a reduction in depth, saving in steel weight and rapid construction program.

Composite action enhances structural efficiency by combining the structural elements to create a single composite member. Composite steel-concrete construction is a very interesting option for structural engineers, but the behavior of the composite cross sections is enhanced under different types of loading. A fundamental point for the structural behavior and design of composite beams is the level of connection and interaction between the main steel beam and the concrete slab [1].

In the sagging moment zone the optimal use of the composite element occurs, since the concrete is in compression and the steel in tension; the behavioral aspects are well known and many experimental information are available [2,3]. However, since continuous composite beams are commonly used in buildings and bridges, the behavior of hogging moment regions has to be analyzed [4].

Under negative moment the behavior of the composite cross section is reversed (the concrete becomes in tension and the steel in compression). Thus the development of cracking in the slab and the local buckling of the steel profile influence the strength and the ductility of the beam [5]. In this case the structural behavior is very complex due to the interaction phenomena: the bond between the steel reinforcement and the surrounding concrete, and the steel profile-concrete interaction through the type and distribution of mechanical devices.

Furthermore the experimental results concerning composite beams under

negative bending are not many [6, 7] and some phenomena are not yet completely explained. In fact measures are needed to study all the structural aspects in detail; they are related to much localized interactions, thus in some cases their interpretation is not simple.

A fundamental point for the structural behavior and design of composite beams is the level of connection and interaction between the steel section and the concrete slab. The term full shear connection relates to the case in which the connection between the components is able to fully resist the forces applied to it. Whilst this is often assumed in design, it is theoretically impossible and cases where connection has more limited stiffness "Partial interaction" often need to be considered. In this case the connection itself may deform, resulting in relative movement along the steel-concrete interface and the effect of increased shear deformation in the composite beam as a whole.

The use of partial connection provides the opportunity to achieve a better match of applied and resisting moment and some economy in the provision of connectors. Generally, the effects of partial interaction, which are induced by the use of partial shear connection, will result in reduced strength and stiffness, but potential enhancement of overall structural system [8].

It is widely known that laboratory tests require a great amount of time, and are very expensive, but in some cases, they can even be important. On the other hand, finite element method has become, in recent years, a powerful and useful tool for the analysis of a wide range of engineering problems. In the complete investigation of any structural system, the experimental phase is essential. Taking into account the numerical models that should be based on reliable test results, experimental and numerical/theoretical analysis

complement each other in the investigation of a particular structural phenomenon [9].

In order to obtain reliable results up to failure, finite element models must properly represent the constituent parts, adopt adequate elements and use appropriate solution techniques. For instance, the finite elements should permit the study of the sensitivity of response to variability of key component characteristics, including material properties and shear stud layout. Consequently, different spacing in distinct parts of the beam can be adopted, allowing the investigation of partial interaction effects. The present study focuses on the modeling of composite beams with full and partial shear connection using the software ANSYS [10].

## 2. Composite Section

### Kinematic Model

The mechanical phenomena governing the behavior of composite steel-concrete beams can be analyzed, by possible differential equations. The kinematics of the model is shown in Fig. (1.c) and is based on the following hypotheses:

- Slip can occur at the concrete slab steel profile interface.
- Plane section in each component remains plane and perpendicular to the reference axis of the component after deformation. This assumption must be applied separately to the two parts (components) of the composite section (steel profile and concrete slab).
- The two parts (components) of the composite section have (almost) the same rotation and the same curvature if uplift (or separation between the two components) occurs. This assumption is utilized in the approximate calculations of curvature of the composite beam.

Furthermore assumptions are needed in respect to composite section under negative bending, it is assumed that

- The concrete slab is cracked, and the distance between cracks  $d_{cr}$  depends on the geometry of the slab, the mechanical properties and diameter of reinforcing bars [11].
- The concrete between two subsequent cracks is able to bear stresses (tension stiffening effect).
- The reinforcing bars can slip with respect to the surrounding concrete, and the slip is computed at the interface between reinforcement and concrete in tension.
- The generic uncracked section is characterized by a linear distribution of the axial strain, limited to the concrete in compression and the reinforcing bars in tension.

A part of tension can be transferred from steel rebar to surrounding concrete; this transfer is limited to the so-called effective area  $A_{eff}$  [11], which is affected by a constant level of tensile strain.

In Fig.(1) a simple structural scheme representing the support region of a continuous composite beam and the reference axes( x, y, z) are drawn, the origin of the frame is placed in correspondence of the centroid of the composite section.

The distribution of the axial displacements for a given section can be expressed by the function  $u(x, y)$ , which can be defined using the rotation of the section  $\phi$ , the displacement of one of the centroid ( $u_c$  or  $u_s$ ) the slip  $s_1$  between the reinforcing bars and the concrete in tension, and the slip  $s_2$  between the concrete slab and the steel profile.

The differential equations needed to solve the structural problem can be written as a function of the unknown longitudinal displacements of the section.

$$s_1 = u_{sc} - u_{ct} \quad \text{----- (1-a)}$$

$$s_2 = u_s - u_c \quad \text{----- (1-b)}$$

where:

$u_{sc}$  = displacements of reinforcement.

$u_{ct}$  = displacement corresponding to the effective area  $A_{eff}$ .

$u_s$  = longitudinal displacement of the upper fiber of steel beam profile.

$u_c$  = longitudinal displacement of the lower fiber of the concrete slab. The unknown displacement can be used to evaluate the axial strains as follows:

$$\epsilon_s = \frac{du_s}{dx}, \quad \epsilon_c = \frac{du_c}{dx} \quad \text{----- (1-c, d)}$$

$$\epsilon_{sc} = \frac{du_{st}}{dx}, \quad \epsilon_{ct} = \frac{du_{ct}}{dx} \quad \text{----- (1-d, f)}$$

$\epsilon_s$  = strain of the centroid fiber of the steel profile.

$\epsilon_c$  = strain of the centroid fiber of the concrete slab.

$\epsilon_{sc}$  = strain of the steel rebars.

$\epsilon_{ct}$  = strain of the concrete in tension.

To simplify the numerical solution of the problem the six parameters of deformation in equations (1) can be addressed as unknown function of problem. Therefore, six equations are required to solve the problem two of them are kinematics and four are equations of equilibrium.

1. Kinematic equation relating the reinforcing bars and the concrete in tension, in terms of strains,

$$\frac{ds_1}{dx} = \epsilon_{sc} - \epsilon_{ct} \quad \text{---- (2)}$$

2. Kinematic equation relating the strain of the lower fiber of the slab and the one of steel profile in terms of strains and curvature

$$\frac{ds_2}{dx} = \epsilon_s - \epsilon_c + \chi \cdot d \quad \text{---- (3)}$$

where,  $d$  = distance between the two centroid and  $\chi$  = curvature of the section.

3. Equation of equilibrium of the concrete in tension subjected to bond stresses

$$\frac{dT_{ct}}{dx} = n_{sc} \cdot \Omega \cdot \Phi \cdot \tau_b \quad \text{----- (4)}$$

where  $T_{ct}$  = resultant of the tensile stresses acting on the concrete in

tension (it is applied at the centroid of the effective area, because it is affected by constant level of tensile strain);  $\Phi$  diameter of steel rebar,  $n_{sc}$  = number of reinforcing bars; and  $\tau_b$  = bond stress corresponding to the slip  $s_1$ .

4. Equation of translational equilibrium of the concrete slab subjected to interaction force due to shear connectors (Fig.1-b)

$$F_c = F \quad \text{----- (5)}$$

5. Equation of translational equilibrium of the steel beam profile under the interaction force transferred by shear connectors (Fig.1-b)

$$F_s = F \quad \text{----- (6)}$$

6. Equation of rotational equilibrium of the composite section as a whole

$$M = M_s + M_c + F \cdot d \quad \text{----- (7)}$$

These equations together with the constitutive relations can be combined into one differential equation in terms of interface slip ( $s$ ) or the axial force ( $F$ ). The solution can be achieved by finite differences. However, the nonlinear behavior becomes difficult to be considered. A viable technique is by the use of finite elements. This procedure is used in this study with the help of ANSYS.

### 3. Case Study

The simply supported inverted composite steel-concrete beam tested and reported in Ref. [12] was selected for the analysis using the finite element software ANSYS. This beam was loaded by one concentrated load at mid span. The geometry and loading conditions for this case study is detailed as follows:

#### 3.1 Beams And Materials

A typical composite cross section for building construction is considered, as shown in Fig. (2). The steel component of the cross section is a Standard HEB with profile height 180 mm, flange width 180 mm, flange thickness 14 mm and web thickness 8.5 mm. The ratio of width over thickness, both for the flange and the web, fulfils the limits given by

Eurocode 4 [11] for the Class 1 steel sections; thus the profile can be classified as compact, so that full plastic moment and a relevant rotation capacity can be developed.

The concrete slab is 800 mm wide and 120 mm thick, four steel reinforcing bars  $\varnothing 14$  mm are provided. Transverse reinforcement has been also used to reduce local damages due to the action of the shear connectors. Specific tests have been carried out in order to define the stress-strain relationships for structural and reinforcing steel.

Four tests on standard steel specimens extracted from the profile have been performed, and five bars 600 mm long have been tested. The mechanical properties of the steel components are summarized in Table 1.

Three cubic  $150 \times 150 \times 150$  mm concrete specimens have been also tested for each beam, to evaluate the concrete mean compressive strength that was 30MPa.

Casting and curing conditions fitted the real executing processes; subsequently, specimens have been carefully turned upside down before tests, as shown in Fig.(3), to simulate the mechanical behavior of continuous composite beams at the internal supports [13, 14].

A single force has been applied at the beam mid-span using 140 mm wide steel plate in order to spread the load and to reduce local stresses. Web stiffeners of the profile have been installed both at the supports and under the applied load.

### 3.2 The Shear Connection

Headed studs have been provided to ensure the mechanical interaction between the steel profile and the concrete slab required to develop the composite action. They are really the most common devices, since they are cheap and can be installed using fast and reliable welding techniques.

In particular, Fe37k studs, diameter 16 mm, have been used; the arrangement of the shear connectors is given in the

following, and shown in Fig.( 3) for three test beams:

- The beam Type A is characterized by 20 shear studs on a single row, uniformly distributed along the beam (spacing 190 mm);
- The beam Type B is characterized by 20 shear connectors, spaced 190 mm, but concentrated at the ends on two rows, in order to realize a wide zone with constant interaction (shear) force;
- The beam Type C has 8 shear connectors 515 mm spaced, uniformly distributed along the beam.

The beams Type A and B have the same design interaction level, but the arrangement of connectors is quite different; the beam Type C is designed according to partial interaction performance. In order to design the specimens and to define the number of connectors provided at the concrete slab-steel profile interface, Euro code 4 provisions have been considered using partial safety factors equal to 1.

The strength of the shear connectors depends on local complex phenomena of interaction between the concrete and the embedded steel stud; therefore the code provisions suggest setting the ultimate load as the minimum value between the strength of the stud and the resistances of the surrounding concrete. In this case the strength of the shear studs is 60kN. Such a load has been also checked by a push-out test carried out according to Eurocode 4 [11] provisions, obtaining an ultimate load of 73.75 kN.

### 3.3 The Test Set-Up

The experimental tests was carried out using an electro-hydraulic actuator that applied a single force at the mid-span; the displacement control of testing was adopted, so that softening branches of the structural response could be fully analyzed (and visualized).

Many measuring devices were used to record both global parameters, such as rotations and deflections, and local parameters such as strains, slips and

curvatures. To this end potentiometers and inductive transducers were installed to measure the deflection at the mid-span, the rotations at the supports, the crack width in the slab and the slips at the interface between the slab and the steel profile. The set-up of the measuring devices is shown in more details in Figs. (4 and 5).

#### 4. Finite Element Model

##### Software, element types and mesh construction

Advances in computational methods and software have brought the finite element method within reach of both academic researchers and engineers in practice by means of general-purpose nonlinear finite element analysis packages, one of the most used ones nowadays being ANSYS [10]. The program offers a wide range of options regarding element types, material behavior and numerical solution controls, as well as graphics user interfaces (known as GUIs), auto-mesh and sophisticated postprocessors and graphics to speed the analysis.

The finite element types considered in the model are as follows:

- Elastic-plastic shell (SHELL 43 and SOLID 65) elements for the steel section and the concrete slab,
- Nonlinear springs (COMBIN 39) and contact point to point52 (LINK 8). These elements are used to simulate the behavior of the shear connectors in resisting the horizontal shear between the concrete slab and the steel flange.
- Reinforcing bars, both longitudinal and transverse are modeled as smeared in layers throughout the solid 65 (concrete slab) finite elements.

The element **SHELL 43** is defined by four nodes having six degrees of freedom at each node. The element is well suited to model nonlinear, flat or warped, thin to moderately thick shell structures. The six degrees of freedom at each node are translations of the nodes in

x, y, and z-directions and rotations about the nodal x, y, and z-axes. The deformation shapes are linear in both in-plane directions. The element allows for plasticity, creep, stress stiffening, large deflections and large strain capabilities [10]. The element **SOLID 65** is used for three dimensional modeling of solids with or without reinforcing bars (rebars capability). The element has eight nodes and three degrees of freedom (translations) at each node. The concrete is capable of cracking in three orthogonal directions, crushing, plastic deformation, and creep [10]. The rebar are capable of sustaining tensile and compressive forces, but not shear, being also capable of plastic deformation and creep.

The element **COMBIN 39** is a unidirectional element (or nonlinear spring) with nonlinear generalized force-deflection capability that can be used in any analysis. The element has a large displacement capability for which there can be two or three degrees of freedom at each node. The element is defined by two nodes and a generalized force-deflection curve.

**LINK 8** is a spar (or truss) element which may be used in a variety of engineering applications. This element can be used to model trusses, sagging cables, links, springs, etc. The 3-D spar element is a uniaxial tension-compression element with three degrees of freedom at each node: translations of the nodes in x, y, and z-directions. As in a pin-jointed structure, no bending of the element is considered. Plasticity, creep, swelling, stress stiffening, and large deflection capabilities are included. This element is used to simulate the behavior of shear connectors which works as stirrups in resisting the vertical shear at concrete layer and transfer normal force between the concrete and steel flange. The element is defined by two nodes and generalized force-deflection curve and has longitudinal or torsional capability. The longitudinal option is a uniaxial tension-compression element with up to three degrees of freedom (translations) at each node.

For non-linear solution, ANSYS employs "Newton-Raphson" approach to solve nonlinear problems. In this approach, the load is subdivided into a series of load increments. The load increments can be applied over several load steps [10].

A typical finite element mesh for the composite beam is shown in Fig (6). The distribution of shear connectors is meaningful parameter considered in the experimental program. This issue has a relevant interest since the European code [11] allows designing the interaction degree between the components in the composite beams.

Experimental results highlight relevant aspects related to the behavior of composite beams under negative moment such as deflections, cracking, strength, and ductility. Each one of these need detailed analyses and suitable modeling approaches. In the following, the results are briefly discussed and compared to simple theoretical calculations.

### 5. Material Modeling

The modeling of the behavior of composite beams needs taking into account the nonlinear constitutive relationship of the materials (concrete, structural steel, reinforcing steel) and the interaction phenomena (bond between rebar and concrete, force-slip law of connectors).

Von Mises yield criterion with isotropic hardening rule (multi-linear work hardening material) is used to represent the steel beam (flanges and web) behavior. The stress-strain relation is linearly elastic up to yield, perfectly plastic between the elastic limit ( $\epsilon_y$ ) and the beginning of strain hardening and follows the constitutive law for the strain-hardening branch [15];

$$\sigma = f_y E_h (\epsilon - \epsilon_h) \left( 1 - E_h \frac{\epsilon - \epsilon_h}{4(f_u - f_y)} \right) \quad (8)$$

where  $f_y$  and  $f_u$  are the yield and ultimate tensile stresses of the steel component respectively,  $E_h$  and  $\epsilon_h$  are the strain hardening modulus (i.e.,

3500MPa) and the strain at strain hardening of the steel component respectively.

Von Mises yield criterion with isotropic hardening rule is also used for the reinforcing steel bars. An elastic-linear work hardening material is considered, with tangent modulus being equal to 1/10000 of the elastic modulus, in order to avoid numerical problems. The values measured in the experimental tests for the material properties of the steel components (steel beam and reinforcing bars) are used in the finite element analyses.

The concrete slab behavior is modeled by a multi-linear isotropic hardening relationship, using Von Mises yield criterion coupled with an isotropic work hardening assumption. The uniaxial behavior is described by a piece-wise linear total stress-total strain curve, starting at the origin, with positive stress and strain values considering the concrete compressive strength ( $f'_c = 0.8f_{cu}$ ) corresponding to a compressive strain of 0.2%. The stress-strain curve also assumes a total increase in strain of 0.05 in the compressive strength up to the concrete strain of 0.35% to avoid numerical problem due to an unrestricted yielding flow. The concrete element shear transfer coefficients considered are  $\beta_o = 0.2$  (open cracks) and  $\beta_c = 0.6$  (closed cracks). Typical values range from 0 to 1, where 0 represent's a smooth crack (complete loss of shear transfer). The default value of 1 represent's a rough crack (no loss of shear transfer). The default value of 0.6 is used as the stress relaxation coefficient (a device that helps accelerate convergence when cracking is imminent). The crushing capability of the concrete element is disabled to improve convergence.

The concrete tensile strength and Poisson's ratio are assumed as 1/10 of its compressive strength and 0.2 respectively. The concrete elastic

modulus is evaluated according to Eurocode 4[11], i.e.:

$$E_c = 9500(f'_c + 8)^{1/3} \left(\frac{\gamma_c}{24}\right)^{1/2} \quad (9)$$

where,  $\gamma_c$  is equal to 24 kN/m<sup>3</sup>.

The model allows for any pattern of stud distribution to be considered, for instance the conventional uniform arrangement and a triangular spacing scheme where the stud distribution follows the nominal elastic shear force diagram [16]. In all analysis, the number/spacing of studs adopted in the experimental programmers is utilized. The load-slip curves for stud to be used in the analysis were obtained from available push-out tests by defining a table of force values and relative displacements (slip) as input data for the nonlinear springs. These springs are modeled at the steel-concrete interface, as shown in Fig. (7).

### 5.1 Application Of Load And Numerical Control

Concentrated loads are incrementally applied to the model by means of point loads applied at mid-line of concrete nodes on a width of 140mm. The tolerance associated with convergence criterion and the load step increments are varied in order to solve potential numerical problems.

Two limits are established to define ultimate load for each finite element investigation; a lower and an upper bound, corresponding to concrete compressive strain of 0.2% and 0.35% respectively. These two limits define an interval in which the composite beam collapse load is located. A third limit condition is referred to the stud failure point, as defined from the push-out tests.

If the stud failure point is located before the lower bound of concrete, then the mode of failure of the composite beam is considered as being stud failure. Conversely, if the stud failure point is located after the upper bound of concrete, the mode of failure is assumed as being concrete crushing. For the

intermediate case, where the stud failure point lies between the lower and upper bounds of concrete, then the mode of failure could be either of them.

## 6. Experimental-Theoretical Comparison

### 6.1 Load-deflection behavior

Experimental load-deflection curves are reported in Fig.(8), the theoretical results are shown in Fig. (9). The test for the beams Type A and B have been stopped when the deflection was about 300 to 350 mm, while the theoretical results indicate a deflection of about 220 to 240mm, due to clear local buckling resulting in a torsional deformation of the steel beam. The load-deflection curve (experimental and theoretical) of the beam Type C shows a loss of load and deflection corresponding to the fracture of the headed studs that marks the collapse of the connection of the composite system. Local buckling of the steel profile took place too, but occurred after the premature failure of the connectors.

Both experimental and theoretical load-deflection curves show an initial apparent linear trend, after which the reduction of the beam stiffness indicates that yielding occurred. The strain gauges attached on the steel profile and the inductive transducers on the concrete slab allowed recording the development of yielding process; it started in the steel flange under compression and then reached the reinforcement rebars under tension.

The comparison between the load-deflection curves shows a basic agreement between the three curves up to the yielding load. When yielding fully develops, the post-elastic behavior seems to be dependent upon the arrangement of the shear connectors. Local buckling fully developed after yielding of the reinforcement, but the load-deflection curves show an increasing trend even if buckling started due to the steel strain hardening stage.

As the deformation level increases, the load capacity of the beams starts to decrease and a softening branch starts. The latter is steeper in the case of the beam Type B rather than in the case of the beam Type A. This effect is probably due to the stronger restraint of the shear connectors to the steel profile when the uniform distribution is realized, while the absence of devices in a wide zone across the mid-span leads to a greater sensitivity to torsional effects for the beam Type B. The maximum measured strains were about 1%.

### 6.2 Ductility

The beam ductility  $\mu$  could be evaluated as the ratio between the ultimate deflection and the deflection at the yielding  $\delta_y$ . The ultimate deflection could be set according to two different criteria: the deflection at the maximum load ( $\delta_m$ ) and the last deflection measured ( $\delta_u$ ) that corresponds for beams A and B to a loss of load of about 7%. For the beam Type C the ultimate condition is assumed at the connection failure, therefore ( $\delta_m$ ) and ( $\delta_u$ ) are coincident. The values of ductility ( $\mu_m$ ) and ( $\mu_u$ ), respectively corresponding to the two criteria, are summarized in Table 2.

Considering the maximum load condition the result is about the same for all three specimens. If the ultimate condition is assumed, the same ductility is obtained for the beams type A and B, even if the post-elastic behavior and the yielding process are quite different, with much lower ductility of the beam type C limited by the connection failure. Moreover the distribution of connectors along the beam which influences the zone subjected to the maximum interaction force. The distribution of shear connectors that has been chosen for the beam Type B leads to a higher length of the concrete slab subjected to the maximum interaction level than in the beam Type A. The effect of this stress condition is a greater spreading of

yielding in the slab, when the uniform distribution of the shear connectors issued, the zone of the slab subjected to the maximum interaction force is more limited and the yielding is localized around the mid-span. Figs. (10 and 11) show the yielded zone at mid-span respectively for the beams Type A and B at a very high deformation level. For the beam Type C the plastic zone is larger than the extension observed for the beam type A, but the development of plastic processes was limited by the failure of the connectors.

### 6.3 Profile-slab slips

The local measures of slips at the concrete slab-steel profile interface are largely influenced by the connecting device. Fig.(12) reports the distribution of the measured interface slips for each beam, at about 50% of the profile-yielding load. It is easy to recognize that even if the beams Type A and B are characterized by the same interaction degree, slips at the interface are quite different, mainly in the central region of the beam, where shear connectors are not provided in the case of the beam B. When the beam Type C is considered, slips are by far greater than in the other beams, since in this case the shear connection has been designed ensuring a relative small partial interaction.

Fig.(13) reports the distribution of the interface slips measured after yielding of the beams. The plots confirm the above remarks and furthermore point out that shear connectors are more stressed in the case of the beam type C, while the behavior of the beam Type B agrees with that beam A at the support region, where shear connectors have been provided. The relation between the applied load and the slip at the two ends of the beams (left and right support) is shown in Fig. (14). The comparison of the curves shows again the agreement of the measured slips for the beam type A and B, while the beam type C has much larger slips even for low loads. When the load increases the high level stress in the

end connectors of the beam type C is evident; the failure occurred at a slip of about 10 mm that corresponds nearly to the experimental ultimate slip capacity of the studs.

#### 6.4 Profile-slab uplifts

Further results in terms of relative displacements between the two components of the cross section are shown in Fig. (15), the plot gives the differential deflection measured along the beam Type B. In particular the results recorded by the mechanical displacement transducers installed both in the connected region (MSC 4 and 6) and in the region where connectors have not been installed (MSC 1 and 2). It is possible to observe that the connection governs the value of this local parameter, since differential deflections are quite negligible when the connected region is considered, while they strongly increase when the unconnected part of the beam is examined.

Furthermore, it is worth noting that, when the load increases, the differential deflections assume positive and negative values, confirming the torsional effects due to local buckling, especially for the beam type B.

#### 7. Final Remarks

The results for the three beams are not very scattered; the initial experimental stiffness agrees for a short range of load to theoretical uncracked condition, but when cracking occurs the beams stiffness decreases rather rapidly due to progressive cracking of concrete and subsequent increase in slip at interface and yielding of steel.

The experimental stiffness is almost between the composite cracked beam and the stiffness of steel profile. Therefore the comparison points out that the slip of the connecting devices influences the behavior of beams also at serviceability limit state, so that the beam Type C is characterized by the lowest stiffness.

The clear effect of the partial interaction between the concrete slab and

the steel profile, even for beams designed for full interaction, is probably related to the reduction of the stiffness of connectors; it is due to the cracking of the slab that modifies the local dowel action of the studs. The interaction degree is also analyzed in terms of moment curvature relationship. In Fig.(16) the experimental curvature of the steel is plotted within the range measured by the strain gauges and it is referred to a cross section at a distance  $d$  from the mid-span. The experimental results are compared with the theoretical values calculated by assuming full interaction of the profile and the slab, moreover the experimental nonlinear constitutive relationship of the structural and reinforcement steel have been used.

The theoretical model is basically in good agreement with the experimental data; the effect of the connection deformability is clearly shown by the higher stiffness of the theoretical behavior. For what concerns the experimental strength of the beams, the maximum moments are summarized in Table 3, where the plastic moment of the steel profile and of the composite section is also reported, assuming the mean value for the yielding stress of the two types of steel and unitary partial safety factors.

The plastic moment is always attained with the steel hardening process, even for the beam type C where the connection failed prematurely.

#### 8. Conclusions

Experimental tests in Ref. [12] with the analytic of investigations carried out in this study on steel-concrete composite beams have been presented. The results highlighted the following aspects:

- The beams Type A and B, designed for the same level of high interaction, show basically the same response in terms of global parameters (rotations and deflections); however the distribution of the slips and the trend of the differential deflections (uplift) at the steel concrete interface are strictly

dependent upon the arrangement of the connectors;

- The yielded zone in the concrete slab will be extended if shear connectors are installed further apart from the internal support regions in continuous beams;
- The structural behavior of the beam Type C, designed with relatively small partial strength connection, is strongly dependent upon the slip capacity of the connecting devices, since the collapse of the system happens to be due to the fracture of the connection;
- Local buckling develops even if the steel cross section is compact and this local buckling influences the beam behavior in the large post-yielding field;
- The beam stiffness is influenced by the connection deformability even under serviceability conditions, pointing out that the reduction of the stiffness of the shear connectors when the concrete is cracked could not be negligible.
- The plastic bending moment of the cross section has been always reached, also indicated in beam Type C, probably due to over-strength of the studs.

#### References

- [1] Oehlers, D.J. and Bradford, M. A., "Elementary Behavior of Composite Steel and Concrete Structural Members", Butterworth Heinemann, 1999, London, 259 pp.
- [2] Fabbrocino, G., Manfredi G., and Cosenza E., "Non-Linear Analysis of Composite Beams under Positive Bending", *Computers & Structures*, Vol. 70, pp. 77-89, 1999.
- [3] Salari R. M., Spacone E., Shing P.B., and Frangopol D.M., " Non-Linear Analysis of Composite Beams With Deformable Shear Connectors" -ASCE *Journal of Structural Engineering*, Vol.124, No. 10, 1998.
- [4] Aribert, J.M., Xu H., and Ragneau E., (1996), "Theoretical Investigation of Moment Redistribution in Composite Continuous Beam of Different Classes", *Composite Construction in Steel and Concrete III*, ASCE.
- [5] Kemp A.R., Dekker N.W., and Trincherio P. "Differences in Inelastic Properties of Steel and Composite Beams", *Journal of Constructional Steel Research*, No. 34, pp. 187-206, 1995.
- [6] Bode H., Kronenberger H.J., and Michaeli W. "Composite Joints - Further Experimental Results", *Int. Conference Composite Construction Conventional and Innovative*, IABSE, Innsbruck, pp. 433-438, 1997.
- [7] Ramm W., and Elz S., "Behavior and Cracking of Slabs as a part of Composite Beams in Regions with Negative Bending Moments" *Engineering Foundation, Composite Construction in Steel and Concrete III*, ASCE 1996.
- [8] Nethercot D.A., "Effect of Partial Shear Connection in Semi-Continuous Beams", *Advances in structural*, Hancock B. et al. editors, 711 pp., 2003.
- [9] Nethercot D.A., "The Importance of Combining Experimental and Numerical Study in Advancing Structural Engineering Understanding", *Journal of Constructional Steel Research*, No. 58, pp. 1283-96, 2002.
- [10] Swanson Analysis System, ANSYS. Online manual, version 10 software and theory reference.
- [11] Eurocode No. 4, "Common Unified Rules for Composite Steel and Concrete Structures", ENV 1994 -1-I, European Committee for Standardization, Brussels (1992b).
- [12] Fabbrocino, G. and Pecce M., "Experimental Tests on Steel-Concrete Composite Beams Under Negative Bending" *Department of Structural Analysis and Design*, University of Naples *Federico II*, Naples, Italy, 1998.
- [13] Zhu P., Gao X., and Wu Z., "Behavior and Moment Redistribution in Continuous Steel-Concrete Composite Beam", *Proc. of the 3rd Int. Conf. on Steel-Concrete Composite Structures*, ASCCS, pp.425-430, 1991.
- [14] Kemp A.R., Dekker N.W., and Trincherio P., "Differences in Inelastic

Properties of Steel and Composite Beams”, Journal of Constructional Steel Research, No. 34, pp. 187-206, 1995.  
 [15] Gattesco N., “Analysis Modeling of Nonlinear Behavior of Composite Beams With Deformable Connection, Journal of

Constructional Steel Research Vol.22, No. 11, April 1963, pp.269-283.  
 [16] Chapman, J. C., “Experiments on composite beams”, The Structural Engineer, Vol.42, No. 11, November 1964, pp.369-383.

**Table 1: Mechanical properties of reinforcing steel and structural steel.**

	Yielding Stress (MPa)	Ultimate Stress (MPa)	Ultimate Strain (%)
Steel beam	375	474	23.4
Bars	540	635	14

**Table 2: Ductility related parameters.**

	Type A	Type B	Type C
$\delta y$ (mm)	24.9	24.9	25.3
$\delta m$ (mm)	161	160	154
$\delta u$ (mm)	250	289	154
$\mu m$	6.5	6.4	6.1
$\mu u$	10.0	11.6	6.1

**Table 3: Plastic bending moment resistance of beams.**

Steel profile	$M_{p1}$ (kN.m)	$M_{max,exp.}$ (kN.m)		
	Composite	Type A	Type B	Type C
182	216	261	253	248

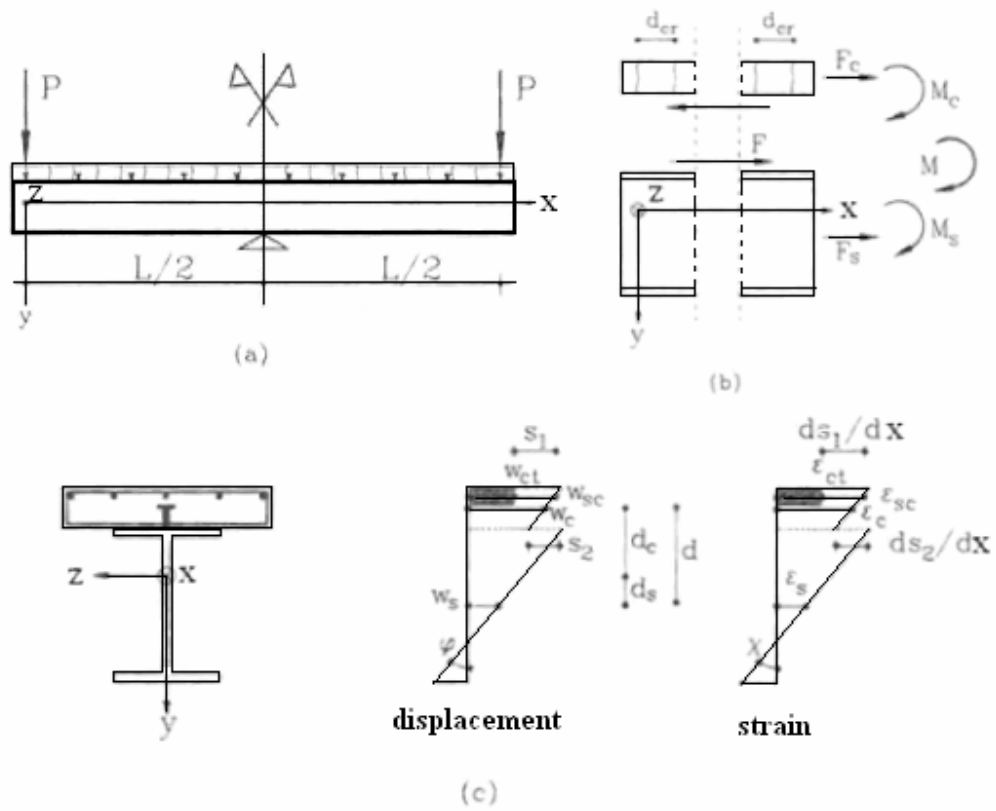


figure. (1) Structural model.

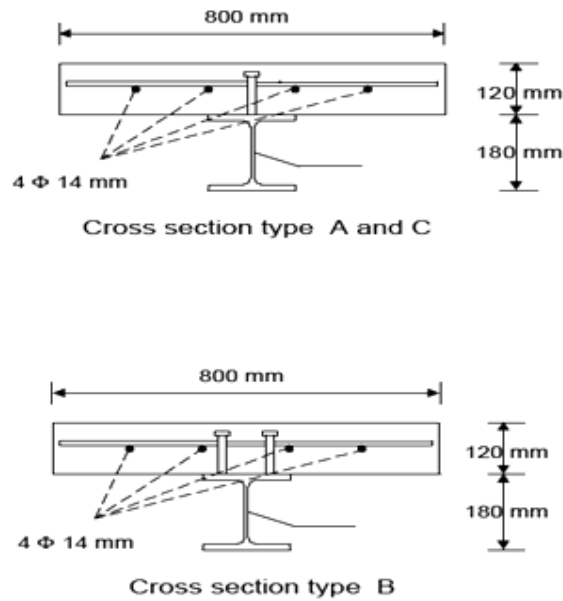


Fig. ( 2) The cross section of the beams.

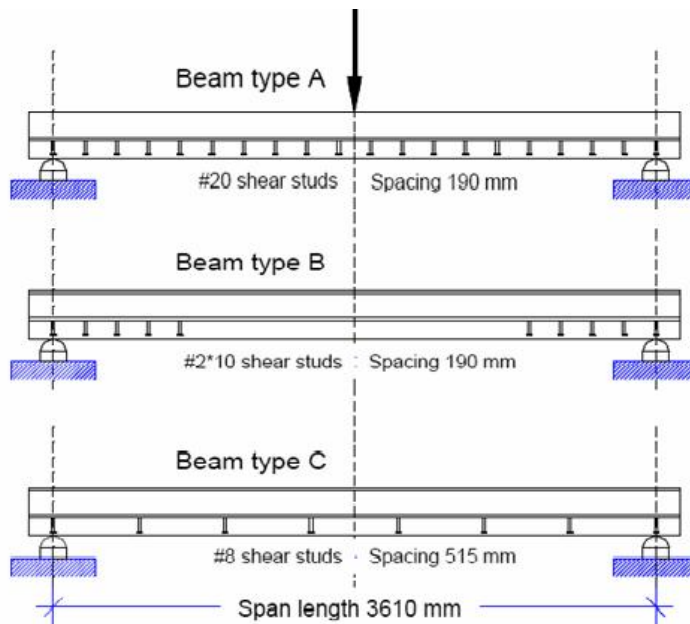


Fig. (3) The load pattern and the arrangement of connectors (beams being inverted)

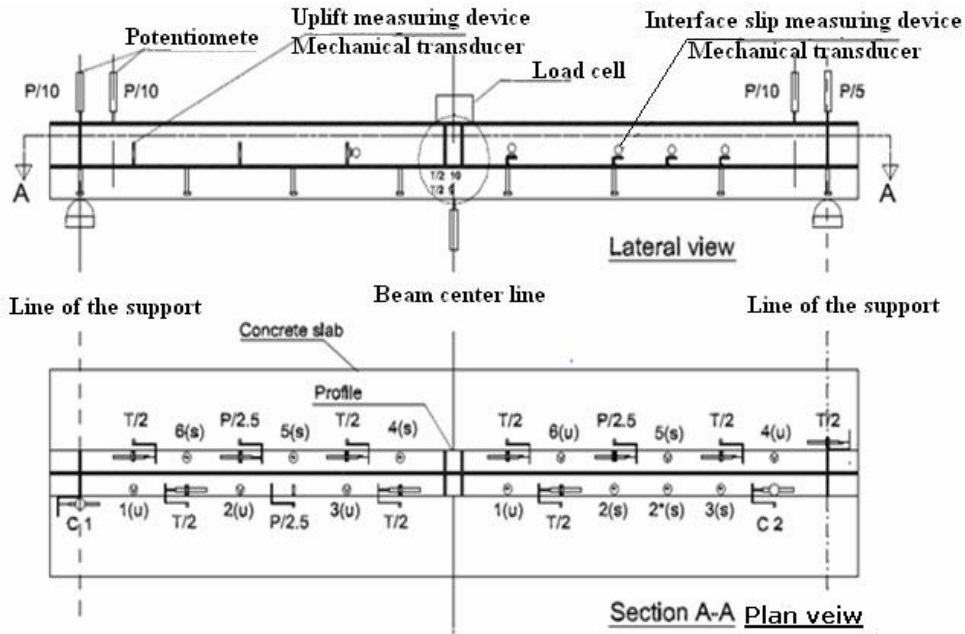


Fig. (4) The set-up of the measuring devices.

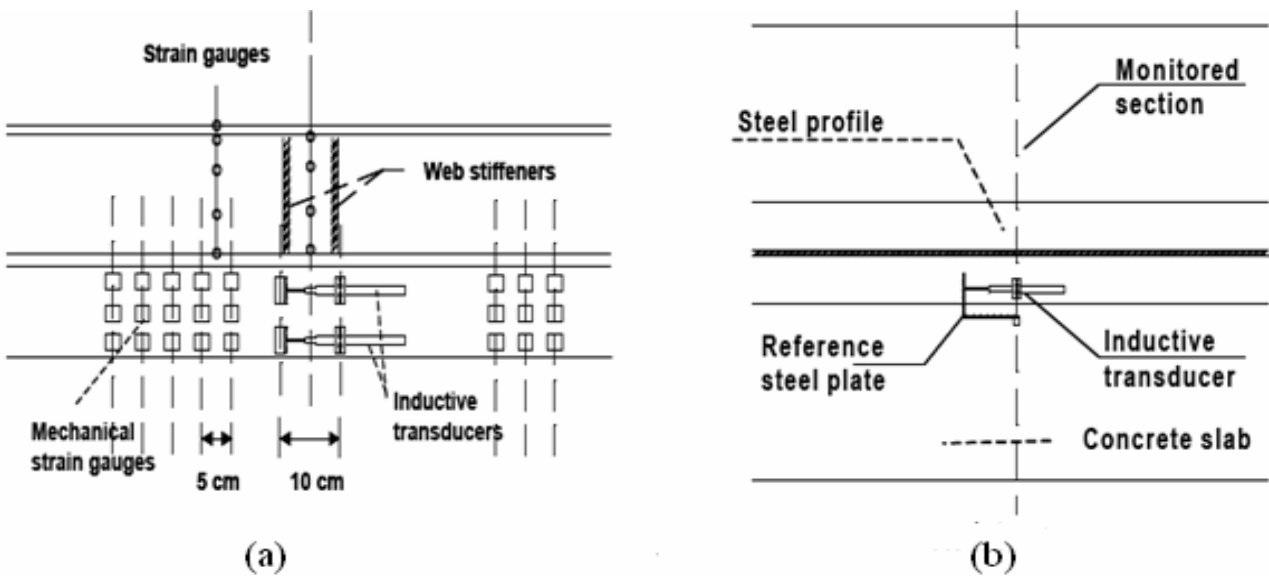


Fig. (5) (a) Details of the measuring devices at mid-span.  
 (b) Steel-concrete interface slip measures.

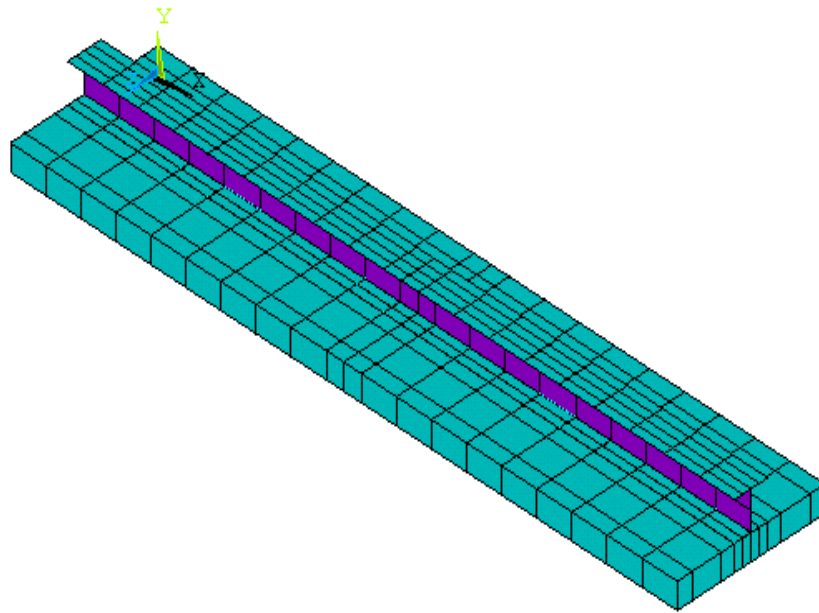
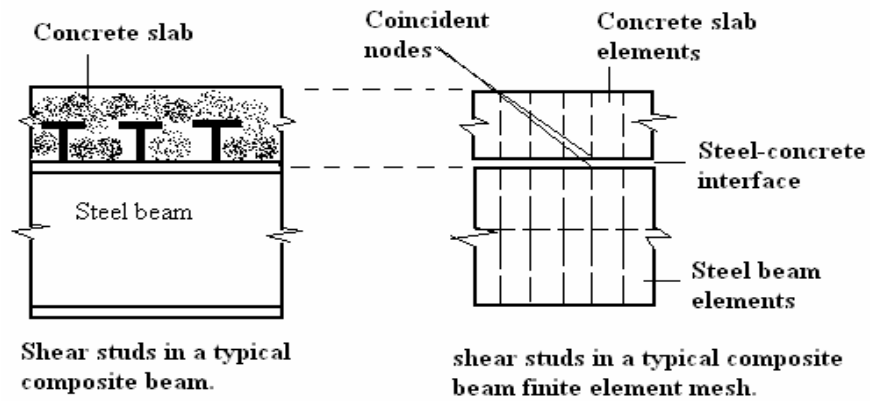
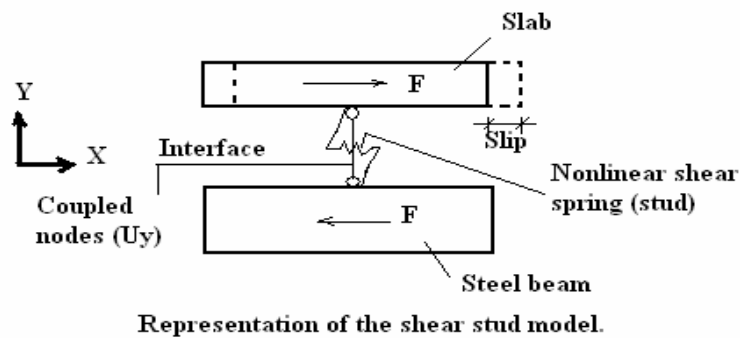


Fig.(6): Typical finite element mesh for composite beam.



Shear studs in a typical composite beam.

shear studs in a typical composite beam finite element mesh.



Representation of the shear stud model.

Fig.(7): Modeling of shear connectors (longitudinal view).

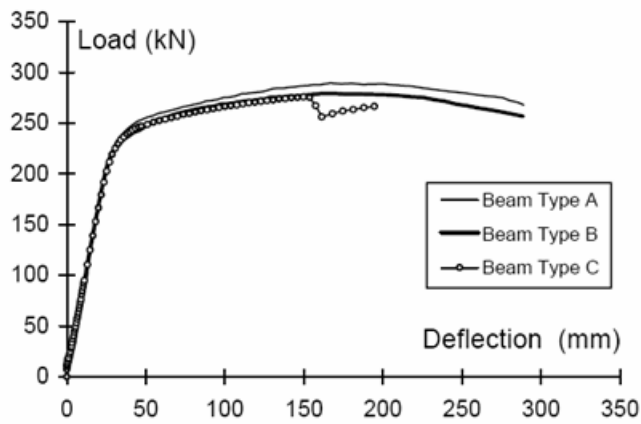


Fig. (8): Experimental mid-span load-deflection curve.

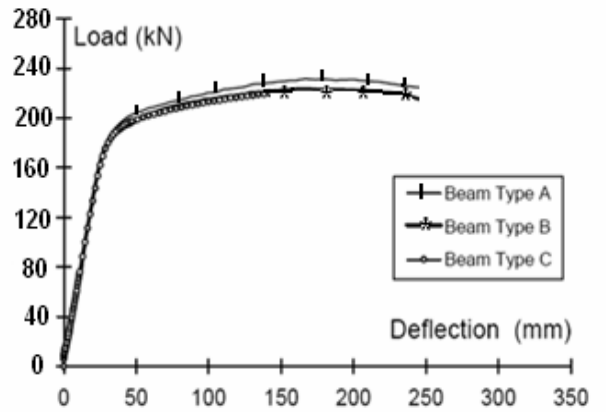


Fig. (9): Theoretical mid-span load-deflection for tested beams.

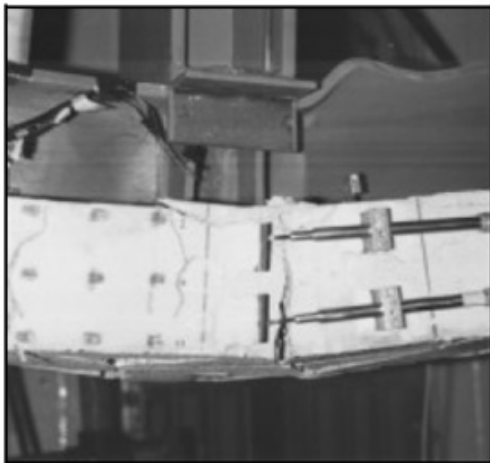


Fig. (10): The beam type A in the post-yielding field.

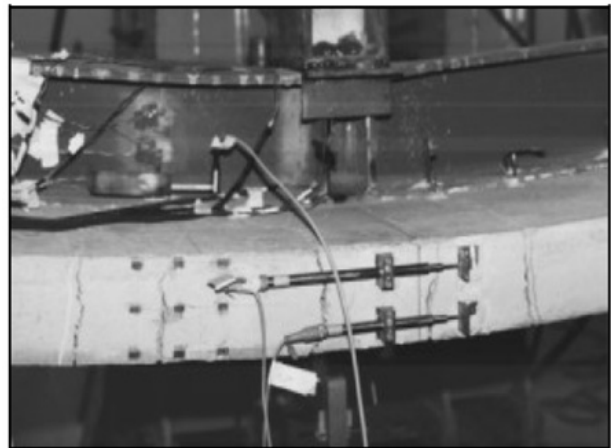


Fig. (11): The beam type B in the post-yielding field.

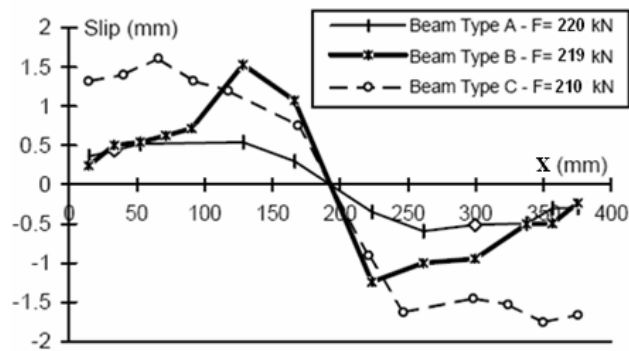


Fig. (12): The profile- slab slips before yielding.

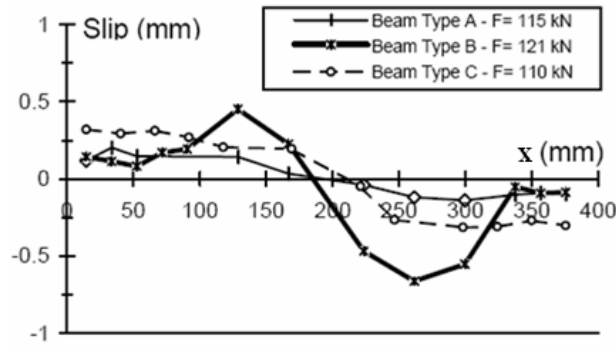


Fig. (13): The profile-slab slips after yielding

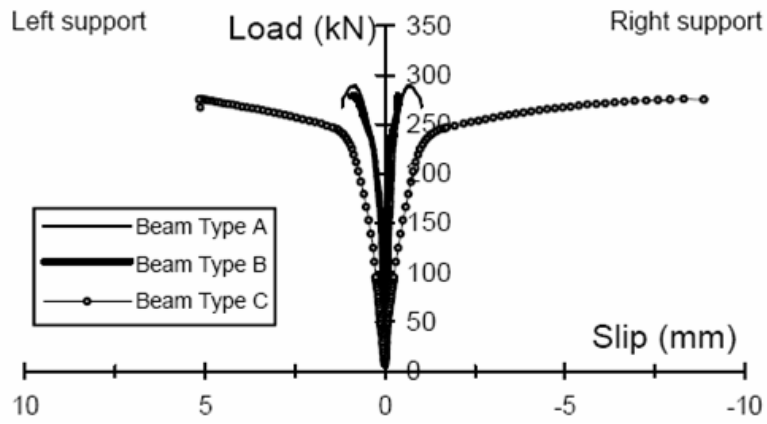


Fig. (14): The slab-profile slips at support.

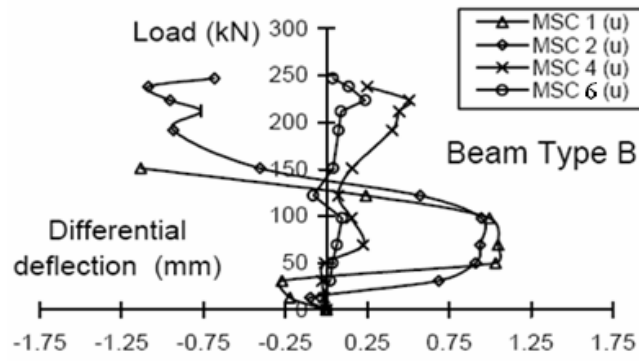


Fig. (15): The differential deflection (uplift).

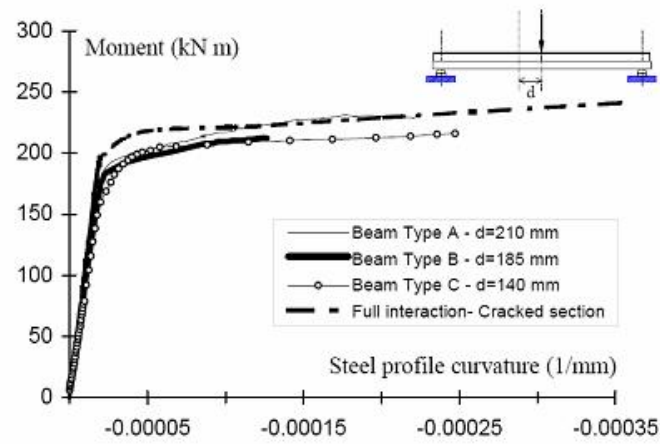


Fig. (16): Experimental moment-curvature relationships compared with the cracked section behavior.